Spectrum Compatibility Analysis Between LEO Navigation Augmentation Signals and GNSS Signals

Sixin Wang, Xiaohui Liu(✉), Xiaomei Tang, Feixue Wang, and Zhaowen Zhuang

College of Electronic Science and Engineering, National University of Defense Technology, Changsha 410073, Hunan, People's Republic of China
luluiu_miter@sina.com

Abstract. Taking advantage of low-earth-orbit (LEO) satellites to establish a LEO navigation augmentation system as a supplement to GNSS is an important development direction in the future. At present, the frequency bands for satellite radio navigation allocated by the International Telecommunications Union (ITU) is quite crowded. BDS, GPS, GLONASS and GALILEO are all overlapped in the L-band. If the signal system of the LEO navigation augmentation system is similar to that of GNSS and occupies the same frequency band, this will inevitably bring the problem of spectrum compatibility. The important parameters of spectrum compatibility evaluation are spectrum separation coefficient, code tracking spectrum sensitivity and effective carrier-power-to-noise-density(C/N_0) degradation, which does not consider the influence of Doppler frequency offset. However, the Doppler frequency offset of LEO navigation signals is relatively large, which will have a great impact on spectrum compatibility evaluation. Therefore, this paper analyzes the influence of large Doppler frequency offset on spectrum compatibility analysis, and simulates the interference of LEO navigation augmentation signals to GNSS signals in L1/E1/B1 frequency band, in which the Doppler frequency offset between LEO navigation satellites and GNSS satellites arriving at the same receiver at different times is considered. The analysis results show that due to the large Doppler frequency offset between signals, the effective C/N_0 degradation of GNSS signals caused by LEO navigation signals is very small, which can be acceptable. By analyzing the spectrum compatibility of LEO navigation augmentation signals and GNSS signals, this paper provides a theoretical basis for the frequency band selection of LEO navigation augmentation system in the future.

Keywords: GNSS · LEO navigation · Spectrum compatibility · Doppler frequency

1 Introduction

Taking advantage of low-earth-orbit (LEO) satellites to establish a LEO navigation augmentation system as a supplement to GNSS is an important development direction in the future. At present, the LEO satellite systems that have been built or are under

C. Yang and J. Xie (Eds.): *China Satellite Navigation Conference (CSNC 2021) Proceedings*, LNEE 773, pp. 114–129, 2021.
https://doi.org/10.1007/978-981-16-3142-9_11

construction including Iridium, Oneweb, O3b, Starlink, etc., will all consider realizing LEO navigation augmentation function and broadcasting LEO navigation augmentation signal (LNAS) [1].

At present, the frequency bands specifically for satellite radio navigation allocated by the International Telecommunications Union (ITU) is quite crowded. BDS, GPS, GLONASS and GALILEO are all overlapped in the L-band. If the signal system of the LEO navigation augmentation system is similar to that of GNSS and occupies the same frequency band, this will inevitably bring the problem of spectrum compatibility. International Committee on Global satellite navigation (ICG) defines "spectrum compatibility" as "assurance that one system will not cause interference that unacceptably degrades the stand-alone service that the other system provides".

The spectrum compatibility analysis between satellite navigation systems starts from the official launch of Galileo system. In 2000, Godet J. proposed for the first time to analyze the spectrum compatibility between satellite navigation systems by using effective carrier-power-to-noise-density (C/N_0) and spectral separation coefficient (SSC) [2]. In the same year, John W. Betz analyzed the narrowband interference of GPS code tracking accuracy, and deduced the above two methods in detail [3]. In 2003, a theoretical analysis method is proposed to analyze the interference in intra-system and inter-system [4]. In 2007, the International Telecommunication Union issued the Recommendation ITU-R M.1831 [5], which is used for frequency coordination among various satellite navigation systems. Soualle F [6, 7] proposed the code tracking spectral sensitivity coefficient (CT-SSC), which is used to evaluate the influence of interference on code tracking process.

In recent years, some domestic researchers have carried out the research work of compatibility. Ran Y studied the compatibility of BDS signals with different modulation modes [8, 9]. Liu W simulated and analyzed all frequency bands of BDS and GPS [10, 11]. Wang Y and others proposed the interference when considering the influence of PRN code, Doppler frequency offset and data rates [12–15]. For the code tracking performance evaluation, Zhai Z studies the code tracking error caused by interference under different conditions [16, 17]. As for the multipath effect, Gan Y, Yang J and Cheng L analyzed the spectrum compatibility with the multipath effect [18–20].

At present, the spectrum compatibility analysis is carried out between GPS, BDS and Galileo, but not between LEO navigation augmentation system and GNSS. Moreover, due to the small Doppler frequency of GNSS, the influence of Doppler frequency offset is hardly considered in the traditional spectrum compatibility evaluation, while the Doppler frequency of the LEO satellite signal is large, which will have a great impact on the spectrum compatibility evaluation and must be taken into account.

Firstly, this paper summarizes the current signal system and constellation parameters of GPS, Galileo and BDS, and analyzes the coincidence of spectrum and power spectral density (PSD) in each frequency band of the three GNSSs. Secondly, the key mathematical model of spectrum compatibility evaluation method is deduced, and the Doppler frequency offset of LNAS is considered. Then, based on this method, the spectrum compatibility between a hypothetical LEO navigation augmentation system with 150 satellites and three GNSSs is simulated and analyzed. Finally, the spectrum compatibility results are discussed comprehensively, which is a theoretical basis for the frequency band selection of LEO navigation augmentation system in the future.

2 Satellite Navigation Signal

2.1 Signal System and Constellation Parameters

Since GLONASS have different multiple access modes than other three GNSSs, this paper only discusses the spectrum compatibility of GPS, Galileo and BDS with LEO navigation augmentation system. Table 1 summarizes the signal system parameters of the three GNSSs. Figure 1 shows the distribution of the navigation signals of the three GNSSs in the frequency band. Note that only civil signals in BDS are shown.

According to the published ICD, the constellation parameters of the three GNSSs are shown in Table 2. Since there is no mature LEO navigation augmentation system, this paper assumes a LEO navigation augmentation system with 150 satellites, whose signal system and constellation parameters are shown in Table 3.

2.2 Signal Model and Real PSD

In order to evaluate the spectrum compatibility more accurately, the real PSD should be given. The receiver baseband signal model can be expressed by

$$s(t) = \sqrt{2C}g(t-\tau_0)D(t-\tau_0)\cos(\Delta\omega_0 t+\varphi_d)+n(t) \tag{1}$$

Where, C is the average received power. $D(t)$ is the transmitted data stream with symbol duration T_d. $\Delta\omega_0$ and φ_d are respectively the residual carrier phase and Doppler frequency after down-conversion. $n(t)$ is the thermal noise. τ_0 is the propagation delay. $g(t)$ is the pulse-modulation code whose expression is

$$g(t) = w(t)\sum_{l=-\infty}^{\infty} c_l\phi(t-lT_c) \tag{2}$$

Where, $w(t)$ is the time window function of length T_d. c_l is the pseudo-random code sequence with period N, code length T_c and pulse shape $\phi(t)$. The PSD of the signal can be expressed as

$$G_s(f) = \frac{1}{T_d}G_d(f)|G(f)|^2 \tag{3}$$

Where, $G_d(f)$ is the PSD of data. Since the data is independent, then $G_d(f) = 1$. From the previous calculations, the PSD for the navigation signal with data modulation can be written as

$$G_s(f) = T_d\left(\frac{1}{NT_c}\right)^2\Phi^2(f)|X_{code}(f)|^2\sum_{k=-\infty}^{\infty}\sin c\left(\pi T_d\left(f-\frac{k}{NT_c}\right)\right)^2 \tag{4}$$

Table 1. Signal system parameters of GPS/GALILEO/BDS

Navigation system	Frequency (MHz)	Navigation signal	Modulation mode		PRN type	PRN rate (Mcps)	PRN code length
GPS	1575.42	L1 C/A	BPSK(1)		Gold	1.023	1023
		L1 Cp	3*TMBOC(6,1,4/33)		Weil	1.023	1800 × 10230
		L1 Cd	1*BOC(1,1)		Weil	1.023	10230
		L1 M	BOCs(10,5)		N/A	5.115	N/A
		L1 P(Y)	BPSK(10)		Compound code	10.23	6.19 × 1012
	1227.6	L2 Cd	BPSK(0.5)	TDDM	Truncation m	1.023	10230
		L2 Cp	BPSK(0.5)		Truncation m		767250
		L2 M	BOCs(10,5)		N/A	5.115	N/A
		L2 P(Y)	BPSK(10)		N/A	10.23	6.19 × 1012
	1176.45	L5I	BPSK(10)	QPSK(10)	Compound code	10.23	10230
		L5Q	BPSK(10)		Compound code	10.23	10230
GALILEO	1575.42	E1PRS	BOCc(15,2.5)		N/A	2.5575	N/A
		E1OSd	CBOC(6,1,1/11)		Random	1.023	4092
		E1OSp			Random	1.023	4092
	1191.795	E5ad	BPSK(10)	AltBOC(15,10)	Gold	10.23	10230
		E5aP	BPSK(10)		Gold	10.23	10230
		E5bd	BPSK(10)		Gold	10.23	10230

(*continued*)

Table 1. (*continued*)

Navigation system	Frequency (MHz)	Navigation signal	Modulation mode		PRN type	PRN rate (Mcps)	PRN code length
		E5bP	BPSK(10)		Gold	10.23	10230
	1278.75	E6CSP	BPSK(5)		Random	5.115	5115
		E6CSd	BPSK(5)		Random	5.115	5115
		E6PRS	BOCc(10,5)		N/A	5.115	N/A
	1561.098	B1I	BPSK(2)		Gold	2.046	2046
	1575.42	B1Cd	BOC(1,1)		Weil	1.023	10230
		B1Cp	QMBOC(6,1,4/33)		Weil	1.023	10230
	1191.795	B2a_d	BPSK(10)	AltBOC(15,10)	Gold	10.23	10230
		B2a_p	BPSK(10)		Gold	10.23	10230
		B2b_I	BPSK(10)		Gold	10.23	10230
		B2b_Q	BPSK(10)		Gold	10.23	10230
	1268.52	B3I	BPSK(10)		Gold	10.23	10230

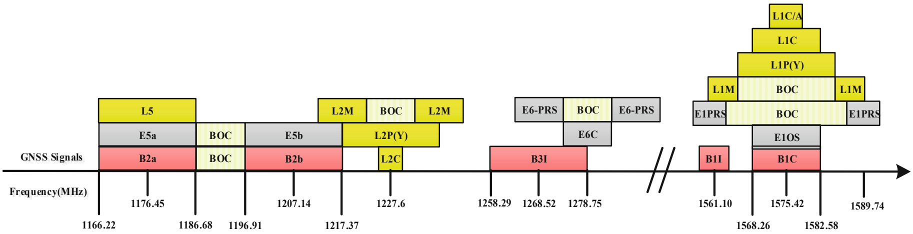

Fig. 1. Frequency distribution of GPS/GALILEO/BDS

Table 2. Constellation parameters of GNSS

Parameter	GPS	GALILEO	BDS
Constellation	Non-Walker (24/6/1 + 3)	Walker (27/3/1)	Walker(27/3/1) + 3IGSO + 5GEO
Inclination	55°	56°	55°(MEO)
Eccentricity	0	0	0
Semi-major Axis	26559.8km	29601.3km	27878km(MEO) 42166.3km(GEO/IGSO)

Table 3. Signals and constellation parameters of LEO navigation augmentation system

Parameter	LEO navigation augmentation system
Modulation mode	BPSK(2)
PRN code type	Gold
PRN code rate	2.046Mcps
PRN code length	2046
Constellation	Walker (120/12/1&30/3/1)
Track inclination	50° (120)/85° (30)
Eccentricity	0
Track radius	7378km

Where, $\Phi(f)$ is the Fourier transform of pulse shape, $X_{code}(f)$ is the code transform, which can be obtained by fast Fourier transform (FFT). Both of them determine the shape of the real PSD. According to different signal types, the other two forms can be derived from Eq. (4)

$$G_s(f) = T_d\left(\frac{1}{NT_c}\right)^2 \Phi^2(f)|X_{code}(f)|^2 \sum_{k=-\infty}^{\infty} \delta\left(\pi T_d\left(f - \frac{k}{NT_c}\right)\right)^2 \tag{5}$$

$$G_s(f) = T_d\left(\frac{1}{NT_c}\right)^2 \Phi^2(f) \tag{6}$$

Taking BDS-B1I as an example, a BPSK modulation is used with a chip rate of 2.046Mcps. PRN code is Gold code with code period 1 ms. Its PSD envelope can be expressed as

$$G_{BPSK}(f) = \frac{1}{f_c}\sin c^2(\frac{f}{f_c}) \tag{7}$$

The real PSD can be obtained from Eq. (4). Figure 2 shows the comparison between the PSD envelope and real PSD of BDS-B1I signal. It can be seen that the maximum difference between them is 30dB, which is caused by the PRN code structure and data rate. Figure 3 shows the enlarged real PSD of B1I signal. It can be seen that it is composed of a series of *sinc* functions, whose interval is 1000 Hz. The PRN code period is 1 ms, so the frequency interval of spectrum line is 1000 Hz.

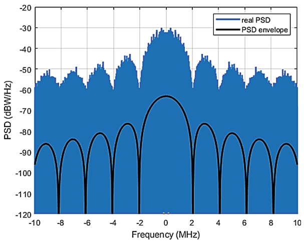

Fig. 2. Comparison between PSD envelope and real PSD of B1I

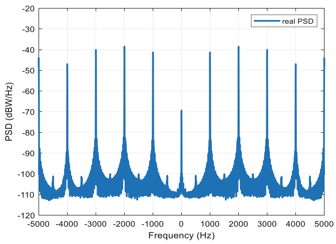

Fig. 3. Enlarged real PSD of B1I

It can be seen from Fig. 2 and Fig. 3 that the PSD envelope is quite different from the real PSD. Therefore, in order to make the analysis results more accurate, the real PSD should be used in the spectrum compatibility evaluation.

2.3 Doppler Frequency Offset Between GNSS Signal and LNAS

Satellites Tool Kit (STK) is used to simulate the Doppler frequency offset between GNSS signal and LNAS. According to the constellation parameters in Table 2 and Table 3, the signal carrier frequency is set to B1 band, the receiver is set in Beijing (41°03′N, 116°20′E), and the simulation time is from 14:00:00 to 20:00:00. The Doppler frequency offset between BDS signal and LNAS at the receiver can be obtained, as shown in Fig. 4. As the number of transit LEO satellites reaches 105 in this period, only 10 of them are selected to be displayed in the figure.

As can be seen from the above figure, the Doppler frequency of BDS signal is within ±5 kHz, while that of LNAS is ±30 kHz. In other words, the maximum Doppler frequency offset between GNSS signal and LNAS is 35 kHz. Moreover, because the moving speed of LEO satellite is very fast, the Doppler change rate of LEO satellite signal is also very fast. Therefore, in the follow-up analysis of spectrum compatibility, in order to make the analysis results more accurate, the Doppler frequency offset of LNAS must be considered.

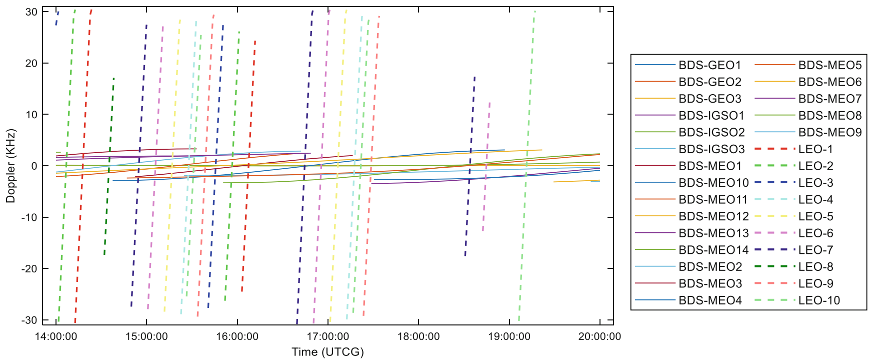

Fig. 4. Doppler comparison between BDS and LNAS

3 Spectrum Compatibility Analysis Method

3.1 Theoretical Formula

SSC represents the correlation between two signals with overlapping spectrum. SSC is related to the modulation type, center frequency, transmitting bandwidth, receiving bandwidth and other parameters of the two signals. SSC is defined as follows[3]:

$$\kappa_{SSC} = \frac{\int_{-\beta_r/2}^{\beta_r/2} G_s(f + f_{dops}) G_j(f + f_{dopj}) df}{\int_{-\beta_r/2}^{\beta_r/2} G_s(f + f_{dops}) df} \tag{8}$$

Where, β_r is the front-end bandwidth of the receiver. $G_S(f)$ and $G_J(f)$ is the normalized PSD of the desired signal and interference signal respectively within the transmission bandwidth. f_{dops} and f_{dopj} is the Doppler frequency of the desired signal and interference signal respectively.

If the spectral peaks of two navigation signals overlap, the SSC will be large, which means that the interference between them will be strong.

Code tracking is not only related to the output of real-time correlator, but also related to the output of delay correlator. When the spectrum overlap between the interference signal and the desired signal is very small, the code tracking error can also be large. Therefore, if we continue to use SSC to evaluate the code tracking performance, it may not be consistent with the real situation. it is inaccurate, or even wrong. Based on this, CT-SSC[7] is proposed as an evaluation method of code tracking. The specific expression is as follows:

$$\kappa_{CT-SSC} = \frac{\int_{-\beta_r/2}^{\beta_r/2} G_s\left(f + f_{dops}\right) G_j\left(f + f_{dopj}\right) \sin^2(\pi f \Delta Tc) df}{\int_{-\beta_r/2}^{\beta_r/2} G_s\left(f + f_{dops}\right) \sin^2(\pi f \Delta Tc) df} \tag{9}$$

Where, Δ is the two-side early-to-late spacing of the receiver correlator (ELS).

Comparing formulas (9) and (8), it can be seen that SSC and CT-SSC differ by a $\sin^2$ function in the integration, which plays a filtering role in the integration. Due to the different overlap degree of interference signal and desired signal with sin2 function, there are differences between SSC and CT-SSC. In addition, different values of Δ will make CT-SSC vary.

According to Recommendation ITU-R M.1831[5], the effective C/N_0 is defined as

$$(C/N_0)_{eff} = \frac{C_s}{N_0'} = \frac{C_s}{N_0 + I_{\text{inter}} + I_{\text{intra}} + I_{\text{ext}}} \tag{10}$$

Where

$$I_{\text{intra}} = \sum_{j=1}^{N_{\text{intra}}} \sum_{i=1}^{M_{\text{intra}}} C_{ij}\kappa_{ij} \tag{11}$$

$$I_{\text{inter}} = \sum_{j=1}^{N_{\text{inter}}} \sum_{i=1}^{M_{\text{inter}}} C_{ij}\kappa_{ij} \tag{12}$$

Where, N_0 is the PSD of noise, C_s is the received desired signal power, C_{ij} is received interfering power of the i-th interfering signal on the j-th satellite, I_{intra} is equivalent white-noise PSD due to aggregate interference from all signals in reference constellation. I_{ext} is equivalent white-noise PSD due to aggregate interference from other systems. M_{intra} and M_{inter} are the number of interfering signals by a satellite in reference constellation and by a satellite in other constellation respectively. N_{intra} and N_{inter} are the number of visible satellite in reference constellation and in other constellation respectively. κ_{ij} is the interference coefficient of desired signal and interference signal, which should be the larger value of SSC and CT-SSC.

Due to the existence of interference signal, the effective noise at the input of the receiver becomes larger. The effective C/N_0 degradation can effectively reflect the degradation of signal performance caused by interference, which is an important parameter to value signal compatibility. The effective C/N_0 degradation caused by intra-system interference is denoted as $\Delta(C/N_0)_{\text{intra}}$, and the effective C/N_0 degradation caused by inter-system interference is denoted as $\Delta(C/N_0)_{\text{inter}}$:

$$\Delta\left(\frac{C}{N_0}\right)_{\text{intra}} = \frac{\frac{C}{N_0}}{\frac{C}{N_0+I_{\text{intra}}}} = 1 + \frac{I_{\text{intra}}}{N_0} \tag{13}$$

$$\Delta\left(\frac{C}{N_0}\right)_{\text{inter}} = \frac{\frac{C}{N_0+I_{\text{intra}}}}{\frac{C}{N_0+I_{\text{intra}}+I_{\text{inter}}}} = 1 + \frac{I_{\text{inter}}}{N_0 + I_{\text{intra}}} \tag{14}$$

3.2 Characteristic Analysis

According to Eq. (8) and Eq. (9), SSC and CT-SSC are related to the PSD, which is directly determined by the parameters of the signal. The analysis shows that the SSC of the navigation signals with short PRN code is greatly affected by data rate, PRN code rate, frequency offset between interference signals and desired signals[13], which cannot be ignored in the analysis of spectrum compatibility.

In addition, the Doppler frequency offset between the interference signal and the desired signal will affect the degree of the PSD overlap between the two signals, which will affect the values of SSC and CT-SSC. The variation of SSC and CT-SSC was analyzed when Doppler frequency offset was within 5 kHz[12]. However, the Doppler frequency difference between the LNAS and GNSS signal can reach up to 35 kHz. Thus, it is necessary to further analyze the influence of large Doppler frequency offset on SSC and CT-SSC.

As can be seen from Fig. 1, the L1/E1/B1 band has the largest number of signals and the most serious spectrum overlap. Therefore, the GNSS civil signals in the L1/E1/B1 band are taken as the desired signals for analysis, including B1Cd and B1Cp of BDS, L1C/A, L1Cp and L1Cd of GPS, E1OSd and E1OS$_p$ of Galileo. Their signal systems are shown in Table 1. The LNAS is interference signal, whose signal system parameters are shown in Table 3, and the carrier center frequency point is set to 1575.42 MHz. The receiving power of all signals is set to -158dBW. The PSD envelope or real PSD, Doppler frequency offset and ELS of each signal are brought into Eqs. (8) and (9) respectively for simulation.

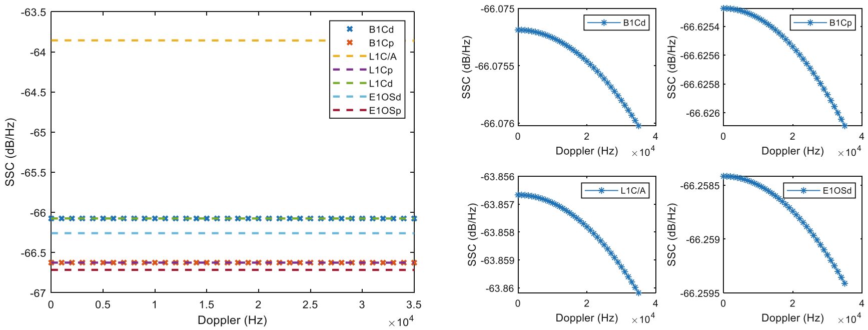

(a) All signals are displayed in one figure **(b) Signals are displayed separately**

Fig. 5. The variation of SSC determined by PSD envelope with different Doppler

From Fig. 5 and Fig. 6, the following conclusions can be drawn.

(1) The SSC determined by the PSD envelope are almost unaffected by Doppler;

(2) The SSC determined by the real PSD vary periodically with Doppler frequency offset, which decreases with the increase of Doppler frequency offset as a whole;

(3) The period amplitude of the SSC of L1C/A is the largest, and the difference between the maximum and minimum values of SSC can be 60 dB. That is to say, L1C/A is the most seriously affected by Doppler frequency offset. The PRN period of L1C/A and LNAS is 1 ms, so the variation period of their SSC is 1 ms. The PRN period of E1OSd and E1OSp is 4 ms, so the variation period of their SSC is 4 ms. The PRN period of B1Cd, B1Cp, L1Cp and L1Cd is 10 ms, so the variation period of their SSC is 10 ms.

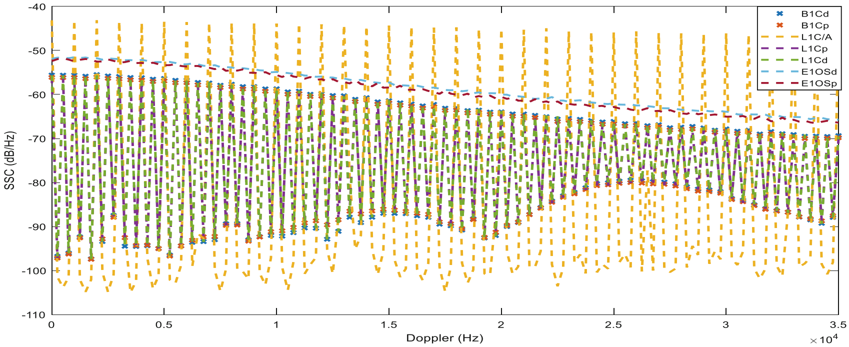

(a) 0Hz≤Doppler≤35KHz, step=250Hz

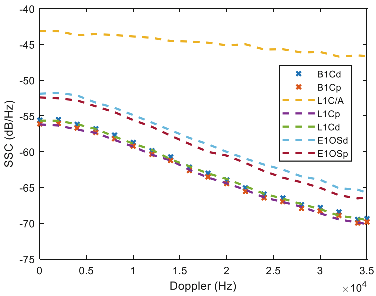

(b) 0Hz≤Doppler≤35KHz, step=2000Hz

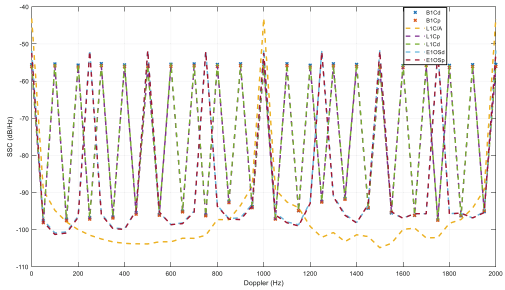

(c) 0KHz≤Doppler≤3000KHz, step=50Hz

Fig. 6. The variation of SSC determined by real PSD with different Doppler offset

Therefore, it can be concluded that the variation period of the SSC equals to the lowest common multiple of their PRN periods.

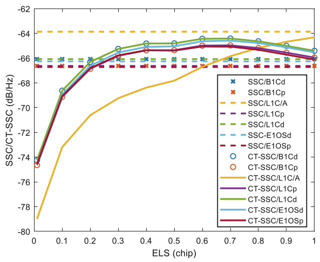

(a) SSC and CT-SSC determined by PSD envelope

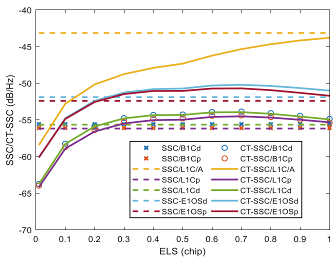

(b) SSC and CT-SSC determined by real PSD

Fig. 7. The relationship between SSC and CT-SSC with different ELS

The following conclusions can be drawn from Fig. 7.

(1) The variation trend of CT-SSC of different signals is the same, where CT-SSC increases with the increase of ELS, and the variation amplitude can reach more than 10dB;

(2) When ELS is small, the value of CT-SSC is always lower than that of SSC, which means in this case, the degradation of code tracking performance caused by interference signal is not as serious as that caused by SNIR.

In conclusion, the spectrum interference between two signals will be significantly affected by Doppler frequency offset, and the values of SSC and CT-SSC are different. Therefore, in order to evaluate the compatibility of LNAS and GNSS more accurately, the average value of SSC and CT-SSC in a period of time considering Doppler frequency offset should be calculated and then the larger value of the two should be taken into the calculation formula of the effective C/N_0 degradation.

4 Simulation Analysis

4.1 Parameter Configuration

In this section, the global interference of LNAS to civil navigation signals of BDS, GPS and Galileo in L1/E1/B1 band is simulated and analyzed. LNAS is the interference signal and GNSS signals is the desired signal. Navigation signal system and constellation parameters are shown in Tables 1, 2 and 3.

In Eqs. (11) and (12), received interfering power of the *i*-th interfering signal on the *j*-th satellite C_{ij} can be expressed by Eq. (15)

$$C_{ij} = \frac{P_{i,j} G_j G_r}{L_{dist} L_{atm} L_{pol}} \tag{15}$$

Where, $P_{i,j}$ is the transmitted power of the *i*-th interfering signal on the *j*-th satellite, G_j is the antenna gain of the *j*-th satellite, G_r is the receiver antenna gain, L_{dist} is the free space propagation loss, L_{atm} is the atmospheric loss, and L_{pol} is the polarization mismatch loss. The simulation parameters in this section are shown in Table 4.

Table 4. Simulation parameters

Parameter	GNSS	LNAS
Simulation time period	1 day	1 day
Time step	60 s	60 s
Grid resolution	5° × 5°	5° × 5°
Elevation angle	15°	15°
Emission bandwidth	30.69 MHz	30.69 MHz
Front end bandwidth	24 MHz	24 MHz
Thermal noise	−204 dBW	−204 dBW
Atmospheric loss	1 dB	1 dB
Polarization mismatch loss	1 dB	1 dB
Transmitted power	26 W	0.05 W
Receiver antenna gain	0 dB	0 dB

Figure 8 shows the constellation map of LEO navigation augmentation system by constellation parameters in Table 3, and Fig. 9 shows the satellites coverage of LEO navigation augmentation constellation. It can be seen from the figure that the Leo navigation augmentation system composed of 150 LEO satellites can achieve triple coverage at most in the world.

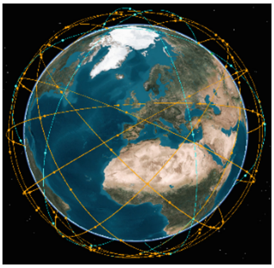

Fig. 8. Constellation map of LEO navigation augmentation system

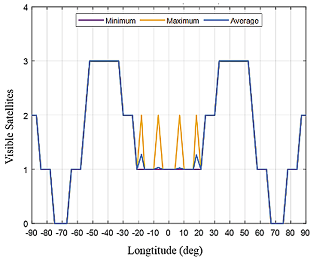

Fig. 9. Satellites coverage of LEO navigation augmentation system

4.2 Global Simulation Results

Figure 10, 11, 12 and Fig. 13 shows the global distribution of effective C/N_0 degradation caused by LNAS. The civil signals of BDS, GPS and Galileo in L1 band are the desired signals. The figures on the left show the effective C/N_0 degradation without considering Doppler effect, where the Doppler frequency offset is set to 0 Hz, while the figures on the right considers show the effective C/N_0 degradation with considering Doppler effect, where the Doppler frequency offset is the mean value of the simulation time.

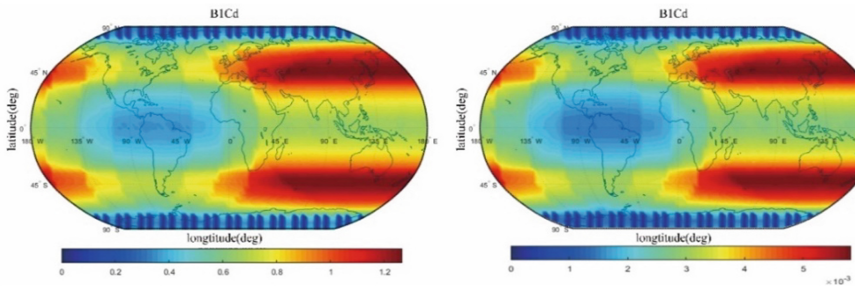

(a)without considering Doppler effect **(b) with considering Doppler effect**

Fig. 10. The distribution of B1Cd C/N_0 degradation caused by LNAS

It can be seen from Fig. 10 to Fig. 13 that.

(1) Compared with the case without considering the Doppler effect, the effective C/N_0 degradation caused by LNAS will be greatly reduced when considering the Doppler effect. Therefore, the traditional spectrum compatibility analysis method without considering Doppler effect will greatly overestimate the interference of LNAS to GNSS signal and draw incorrect conclusions;

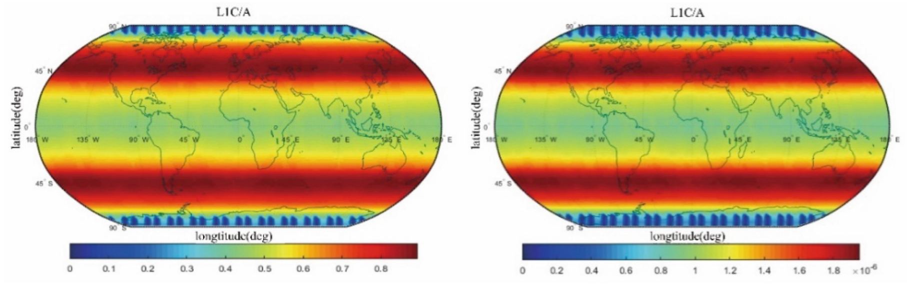

(a)without considering Doppler effect **(b) with considering Doppler effect**

Fig. 11. The distribution of L1C/A C/N_0 degradation caused by LNAS

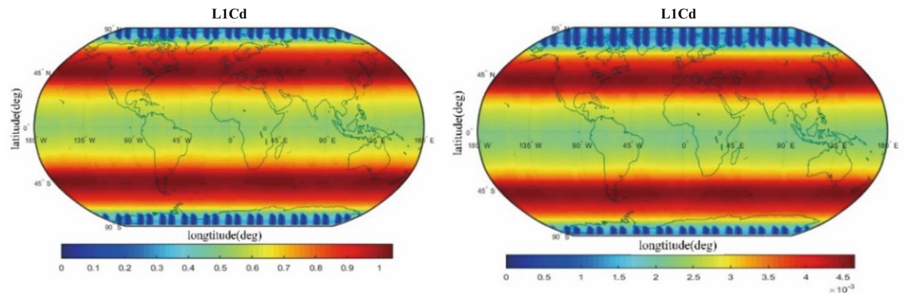

(a)without considering Doppler effect **(b) with considering Doppler effect**

Fig. 12. The distribution of L1Cd C/N_0 degradation caused by LNAS

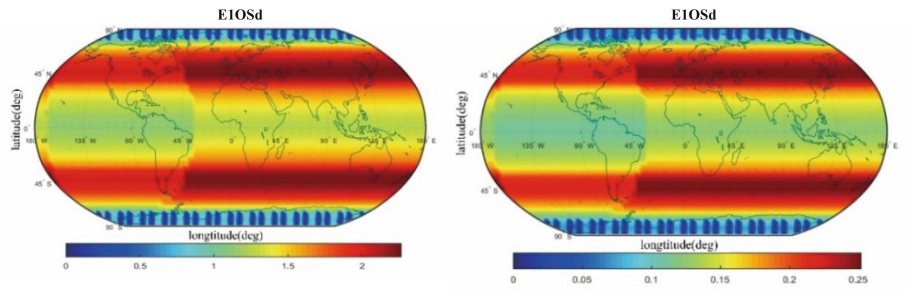

(a)without considering Doppler effect **(b) with considering Doppler effect**

Fig. 13. The distribution of E1OSd C/N_0 degradation caused by LNAS

(2) Considering Doppler effect, the maximum values of effective C/N_0 degradation caused by the interference of LNAS to B1Cd, L1C/A, L1Cd and E1OS are 5.8×10^{-3}dB, 1.8×10^{-6}dB, 4.7×10^{-3}dB and 0.25 dB respectively;

(3) The effective C/N_0 degradation of L1C/A caused by LNAS interference is the smallest, because the SSC of L1C/A and LNAS varies greatly with different Doppler frequency offset (as can be seen from Fig. 9). Therefore, the rapid and huge variation of Doppler frequency offset caused by the rapid movement of LEO satellite leads to the

rapid and huge variation of LNAS interference to L1C/A. The figure shows the average value in one day, which means the average interference of LNAS to L1C/A in one day is the least;

(4) The effective C/N_0 degradation of E1OSd caused by LNAS interference is the largest, because the received power of E1OSd is lower than other GNSSS signals, so it is most heavily affected by LNAS;

(5) The effective C/N_0 degradation of B1Cd and L1Cd caused by LNAS interference is similar, which is due to the same modulation mode and spectrum of B1Cd and L1Cd;

(6) The effective C/N_0 degradation of BDS signal is different from that of Galileo and GPS signal, which is due to GEO and IGSO satellites in BDS;

In general, when the number of LEO satellites is 150, and the transmitted power of LEO satellite is small, where the landing power is close to the landing power of GNSS signal, the interference of LNAS to GNSS signal is very small, which is acceptable.

5 Conclusion

With the construction of LEO satellite system and the broadcast of LEO navigation augmentation signal, more and more signals will share L-band. The spectrum interference from LEO satellite to the existing GNSS is inevitable. The important parameters of traditional spectrum compatibility evaluation are SSC, CT-SSC and effective C/N_0 degradation, which do not consider the influence of Doppler frequency offset. The large Doppler frequency offset of LEO navigation signal will have a great impact on spectrum compatibility evaluation, so it must be taken into account. Firstly, this paper summarizes the current signal system and constellation parameters of GPS, Galileo and BDS, and analyzes the PSD envelope and spectrum overlap of each frequency band. In addition, a LEO navigation augmentation system with 150 satellites is assumed, with its signal system and constellation parameters. Secondly, the key mathematical model of compatibility evaluation method is analyzed. Then, based on this method, considering the constellation, transmit power, elevation and Doppler frequency offset of the satellite navigation system, the spectrum compatibility between LNAS and three GNSS signals in the L1/E1/B1 band is simulated and analyzed. The simulation results show that the interference degree of LNAS to GNSS signal in L1/E1/B1 band is very small, which is acceptable. This is due to the large Doppler frequency offset between LEO navigation augmentation signal and GNSS signal. In the future, we can continue to analyze the spectrum compatibility between LNAS and GNSS signal with different number of LEO satellites and different signal systems. Moreover, we can find the frequency band with the least interference caused by LEO navigation augmentation by analyzing the spectrum compatibility of GNSS signals in all frequency bands.

Acknowledgments. This study is supported by National Nature Science Foundation of China U20A0193 and 62003354.

References

1. Lu, J., Guo, X., Su, C.: Global capabilities of BeiDou navigation satellite system. Satell. Navig. **1**, 27 (2020)

2. Godet, J.: GPS/Galileo radio frequency compatibility analysis. In: ION GPS 2000, Alexandria, VA, pp. 1782–1790 (2000)
3. Betz, J.W., Fine, E.B.: Effect of narrowband interference on GPS code tracking accuracy. In: Proceedings of the 2000 National Technical Meeting of the Institute of Navigation, Long Anaheim, CA, pp. 716–723 (2000)
4. Titus, L.B.M., Betz, J.W., Hegarty, C.J., et al.: Intersystem and intrasystem interference analysis methodology. In: ION GNSS 2003, Alexandria, VA, pp. 2061–2069 (2003)
5. A coordination methodology for RNSS inter-system interference estimation. Recommendation ITU-R M.1831 (2007)
6. Soualle, F.: Introduction an additional radio frequency compatibility criterion for code tracking performance. In: ESTEC GNSS Signals, pp. 1–8 (2007)
7. Soualle, F.: Radio frequency compatibility criterion for code tracking performance. In: ION GNSS 2007, Alexandria, VA, pp. 1201–1210 (2007)
8. Ran, Y., Hu, X., Liu, Y., Tang, Z.: Compatibility of compass navigation signals. Chin. Sci. Phys. Mech. Astron. **40**(05), 676–684 (2010)
9. Ran, Y., Hu, X., Ke, J., Yi, L.: Compatibility of satellite navigation signals under different modulation modes. In: CSNC 2nd China Satellite Navigation Symposium, Shanghai (2011)
10. Liu, W.: Research on the overall technology of GNSS compatibility and interoperability. Doctoral dissertation of Shanghai Jiaotong University, Shanghai (2011)
11. Liu, L., Zhan, X., Liu, W., Niu, M.: Beidou satellite navigation system and its application GPS compatibility evaluation. J. Surv. Mapp. **5** (2011)
12. Wang, Y., Yang, S., Yu, B., et al.: Interference analysis and simulation for GPS/Galileo signals. In: International Conference on Mechatronics and Automation, ICMA 2009. IEEE (2009)
13. Wang, Y., Wei, B., Luo, X., et al.: Research on GNSS compatibility method. Syst. Eng. Electron. Technol. **32**(6), 1305–1308 (2010)
14. Wang, Y., Wei, B., Luo, X., Wang, J.: Theoretical research and simulation analysis on GNSS compatibility. In: Electronic Proceedings of the 2nd China Satellite Navigation Academic Annual Meeting (2011)
15. Wang, G., Wang, J., Luo, X., Wei, B.: Research on GNSS compatibility analysis method of CT-SSC. In: Proceedings of the First China Satellite Navigation Academic Annual Meeting, no. 2 (2010)
16. Zhai, Z., Yang, J., Yang, J.: Analysis of PN code tracking error under partial band interference. J. Natl. Defense Univ. Sci. Technol. (2015)
17. Zhai, Z., Yang, J., Yang, J.: Research on PN code tracking error caused by single product interference under large error condition. Acta electronica Sinica **1** (2016)
18. Gan, Y., Zhou, Y.: Multipath suppression performance analysis of GNSS signal multi gate delay structure. Telecommun. Technol. **54**(7), 905–909 (2014)
19. Yang, J., Jin, T., Huang, Z., et al.: Non envelope evaluation method for multipath error of GNSS signal. J. Wuhan Univ. **2** (2016)
20. Cheng, L., Chen, J., Xie, G.: Modeling and analysis of GPS carrier tracking error. J. Beijing Univ. Technol. (2014)